JOURNAL OF TISSUE ENGINEERING AND REGENERATIVE MEDICINE
J Tissue Eng Regen Med 2018; **12**: e962–e972.
Published online 31 May 2017 in Wiley Online Library (wileyonlinelibrary.com) **DOI:** 10.1002/term.2418

RESEARCH ARTICLE

Adipose-derived perivascular mesenchymal stromal/stem cells promote functional vascular tissue engineering for cardiac regenerative purposes

Justin Morrissette-McAlmon[1,2], Adriana Blazeski[2], Sarah Somers[1,2], Geran Kostecki[2], Leslie Tung[2] and Warren L. Grayson[1,2,3,4]*

[1]*Translational Tissue Engineering Center, Johns Hopkins University School of Medicine, Baltimore, MD, USA*
[2]*Department of Biomedical Engineering, Johns Hopkins University School of Medicine, Baltimore, MD, USA*
[3]*Department of Material Sciences & Engineering, Johns Hopkins University, School of Engineering, Baltimore, MD, USA*
[4]*Institute for Nanobiotechnology (INBT), Johns Hopkins University School of Engineering, Baltimore, MD, USA*

Abstract

Cardiac tissue engineering approaches have the potential to regenerate functional myocardium with intrinsic vascular networks. This study compared the relative effects of human adipose-derived stem/stromal cells (hASCs) and human dermal fibroblasts (hDFs) in cocultures with neonatal rat ventricular cardiomyocytes (NRVCMs) and human umbilical vein endothelial cells (HUVECs). At the same ratios of NRVCM:hASC and NRVCM:hDF, the hASC cocultures displayed shorter action potentials and maintained capture at faster pacing rates. Similarly, in coculture with HUVECs, hASC:HUVEC exhibited superior ability to support vascular capillary network formation relative to hDF:HUVEC. Based on these studies, a range of suitable cell ratios were determined to develop a triculture system. Six seeding ratios of NRVCM:hASC:HUVEC were tested and it was found that a ratio of 500:50:25 cells (i.e. 250,000:25,000:12,500 cells/cm^2) resulted in the formation of robust vascular networks while retaining action potential durations and propagation similar to pure NRVCM cultures. Tricultures in this ratio exhibited an average conduction velocity of 20 ± 2 cm/s, action potential durations at 80% repolarization (APD_{80}) and APD_{30} of 122 ± 5 ms and 59 ± 4 ms, respectively, and maximum capture rate of 7.4 ± 0.6 Hz. The NRVCM control groups had APD_{80} and APD_{30} of 120 ± 9 ms and 51 ± 5 ms, with a maximum capture rate of 7.3 ± 0.2 Hz. In summary, the combination of hASCs in the appropriate ratios with NRVCMs and HUVECs can facilitate the formation of densely vascularized cardiac tissues that appear not to impact the electrophysiological function of cardiomyocytes negatively.

Received 22 August 2016; Revised 18 December 2016; Accepted 16 January 2017

Keywords **Cardiac tissue engineering; vascularized grafts; Adipose-derived stem cells; dermal fibroblasts; electrophysiology; Neonatal rat ventricular cardiomyocytes**

1. Introduction

Cardiac tissue engineering is a promising approach to regenerate the damaged myocardium. The native myocardium is composed of many different cell types that all play a specific role in the functionality and survival of the organ. These cell types include cardiomyocytes, endothelial cells and fibroblasts (Hirt *et al.*, 2014; Lesman *et al.*, 2010). Although cardiomyocytes account for the largest volume of cells at 80–90% (Tandon *et al.*, 2013), supporting cell types account for the largest number of cells (Jackman *et al.*, 2015; Kohl *et al.*, 2005). Endothelial cells, which are primarily responsible for blood vessel development, provide the heart with nutrient and oxygen supply through the coronary vasculature (Brutsaert, 2003). In addition to dense vessel networks, the heart has a large population of fibroblasts. Fibroblasts have been shown to make up >50% by number of the cellular population in the adult mammalian heart (Porter and Turner, 2009). Fibroblasts maintain the mechanical properties of the heart, provide the structure of the extracellular matrix and produce growth factors (Baum and Duffy, 2011; Kohl *et al.*, 2005; Takeda *et al.*, 2010).

Previous studies have shown that using the native cellular makeup for cardiac muscle improves cardiomyocyte survival, force of contraction and maximum capture rate of engineered grafts and promotes vascular development for possible anastomosis with host vasculature to provide prolonged survival (Caspi *et al.*, 2007; Lesman *et al.*, 2010). A delicate balance of cellular ratios is necessary to develop vascularized cardiac tissue that is able to maintain normal electrophysiological function while developing robust vascular structures (Brutsaert, 2003; Kawamura *et al.*, 2013).

Fibroblasts have traditionally been excluded from cultures of neonatal rat ventricular cardiomyocytes (NRVCMs) as they can impede and/or alter the electrophysiological function (e.g. action potential conduction) of cardiomyocytes (Thompson *et al.*, 2014). However, fibroblasts also provide mechanical and

*Correspondence to: Warren L. Grayson, Johns Hopkins University, Department of Biomedical Engineering, Translational Tissue Engineering Center, 400 North Broadway, Smith Building 5023, Baltimore, MD 21231, USA. E-mail: wgrayson@jhmi.edu

biochemical support and have at times been intentionally included in cocultures with cardiomyocytes (Liau *et al.*, 2011). Previous tricultures have used fibroblasts from lung or foreskin as a means to stabilize the nascent vasculature formed by endothelial cells (Iyer *et al.*, 2009a, b). The source of the fibroblast impacts the levels of proangiogenic factor secretion (Chen *et al.*, 2010). In several studies, mesenchymal stem cells have served as fibroblast replacements (Freiman *et al.*, 2016). Bone marrow-derived mesenchymal stem cells can be an attractive cell source, but isolations are painful and result in low cell yields. Bone marrow-derived mesenchymal stem cells have been shown to aid in the stabilization of vasculature in the presence of endothelial cells, but when cocultured with cardiomyocytes have been shown to fuse and reduce the electrophysiological properties of cardiomyocytes (Poll *et al.*, 2008; Shadrin *et al.*, 2015). Consequently, there is a need for a cell population that has the potential to act as vascular mural cells (Koh *et al.*, 2011) and does not significantly inhibit the electrical functioning of cardiomyocytes.

Human adipose-derived stem/stromal cells (hASCs) are a clinically relevant stem cell source that is of mesodermal origin and are available in large quantities upon isolation. They have the ability to differentiate into vascular mural cells (Hutton *et al.*, 2012; Merfeld-Clauss *et al.*, 2010), and form gap junctions with electrically excitable cells allowing the electrical signal to propagate across and trigger calcium transients (Choi *et al.*, 2010). The hASCs in coculture with endothelial cells display a pericyte-like phenotype, ultimately stabilizing newly-formed vascular networks (Merfeld-Clauss *et al.*, 2010, 2014). Crisan and colleagues have shown that cells derived from white adipose tissue can display perivascular markers such as CD146, α-SMA and NG2, and showed negative expression of endothelial markers CD31 and CD144 (Corselli *et al.*, 2013; Crisan *et al.*, 2008, 2012). They also have the ability to withstand temporary ischaemia, release trophic and paracrine factors, and prevent inflammation (Blasi *et al.*, 2011; Yoshimura *et al.*, 2009). These properties of hASCs suggested that it might be beneficial to assess their role as fibroblast replacements in coculture with NRVCMs and human umbilical vein endothelial cells (HUVECs).

This study was conducted to determine the potential benefits of using hASCs relative to dermal fibroblasts to provide vascular stabilization while maintaining the electrophysiological properties of cardiomyocytes in a triculture system. In the development of a vascularized cardiac tissue, prior studies have demonstrated that tricultures (cardiomyocytes, endothelial cells and fibroblasts) exhibit significantly better outcomes with the development of stabilized vasculature structures, decreased excitation threshold, and maintenance of maximum capture rate relative to enriched cardiomyocyte populations and coculture systems in which cardiomyocytes and endothelial cells alone were used (Iyer *et al.*, 2009a, b). The functional outcomes of cocultures of varying ratios of NRVCM:hASC [(and NRVCM:human dermal fibroblasts (hDFs)] were assessed in a well-established monolayer model using optical recordings of transmembrane voltage. The effect of the ratio of hASC:HUVEC (and hDF:HUVEC) on vessel length and interconnectivity was also evaluated. This information was used to develop a triculture system with a ratio of NRVCM:hASC:HUVEC that incorporated the benefits of hASCs for vascularized cardiac regeneration while maintaining the electrophysiology of enriched cardiomyocyte cultures.

2. Materials methods

2.1. Isolation of hASCs

Isolation of hASCs was performed at the Stem Cell Biology Laboratory, Pennington Biomedical Research Center, under an Institutional Review Board approved protocol according to published methods (Dubois *et al.*, 2008). Briefly, fresh human subcutaneous adipose lipoaspirates were obtained under informed consent from healthy Caucasian female donors with a mean age of 47.6 ± 1.9 years and mean body mass index of 27.1 ± 0.6 and undergoing elective liposuction surgery. The lipoaspirate tissue was extensively washed with warm Dulbecco's phosphate-buffered saline solution (DPBS) to remove erythrocytes and then digested in DPBS supplemented with 0.1% Collagenase Type I (Worthington), 1% bovine serum albumin, and 2 mM $CaCl_2$ for 1 h at 37°C. Following room temperature centrifugation at 300 *g* and suspension in stromal medium [Dulbecco's modified Eagle's medium (DMEM)/F-12 (Life Technologies) supplemented with 10% fetal bovine serum (FBS; Atlanta Biologicals) and 1% penicillin/streptomycin], the stromal vascular pellet obtained from 35 mL of digested lipoaspirate was plated in a T175 flask (0.2 mL per cm^2). After 24 h of incubation at 37°C, 5% CO_2, the adherent cells were washed with warm DPBS and maintained in stromal medium until reaching 80–90% confluency. The adherent population (passage 0) was harvested by digestion with trypsin with 0.05% ethylenediamine tetra-acetic acid (1 mM) at 37°C for 5 min, washed with stromal medium, and cryopreserved for shipment to Johns Hopkins University. Prior studies have shown that there are no deleterious effects on hASCs due to cryopreservation, such as loss of viability or multipotency (Dubois *et al.*, 2008). For expansion, hASCs were thawed and cultured in expansion medium, which consists of DMEM high glucose (Life Technologies), 10% FBS (Atlanta Biologicals), 0.5% penicillin/streptomycin (Cellgro), 0.5% antibiotic/antimycotic, 1 ng/mL fibroblast growth factor-2 (bFGF/FGF-2; PeproTech). Cells were used at passage 4 (P4) to minimize contamination of heterogenic cell types.

2.2. Isolation of neonatal rat ventricular cardiomyocytes

All procedures with animals were completed in accordance with the regulations set forth by the Johns Hopkins Committee on Animal Care and Use along with all state and federal regulations. In brief, NRVCMs were

enzymatically dissociated from the hearts of 1–3-day-old Sprague–Dawley rats (Charles River Laboratories, Frederick, MD, USA) as previously described (Blazeski *et al.*, 2015; Toraason *et al.*, 1989). Freshly isolated cells were suspended in NRVCM culture media [Medium 199 (Life Technologies), 1% HEPES buffer solution (Life Technologies), 1% MEM nonessential amino acids (Life Technologies), 2 mM L-glutamine (Life Technologies), 20 μM glucose (Sigma Aldrich), 4 μg/mL Vitamin B_{12} (Sigma Aldrich), 1% Penicillin (Cellgro), and 10% or 2% heat-inactivated FBS (Sigma Aldrich)] and preplated in flasks twice, for 1 h each time in order to reduce the proportion of fibroblasts.

2.3. HUVEC culture

A vial of pooled HUVECs (Lonza) were expanded in tissue culture flasks up to passage 4 or 5 using endothelial basal medium 2 culture medium (Lonza, USA) supplemented with the endothelial growth medium-2 (EGM-2) bullet kit [hydrocortisone, human FGF-2, vascular endothelial growth factor (VEGF), R3-insulin-like growth factor-1, ascorbic acid, human epidermal growth factor, gentamicin–amphotericin (GA-1000), and heparin] and 2% FBS. HUVECs were used for experimentation at Passage 5-6.

2.4. Fibroblast expansion and characterization

The hDF-BJ cell line (ATCC) was expanded in tissue culture flasks up to passage 5 (P5) using DMEM (Life Technologies), 10% FBS (Atlanta Biologicals), and 0.5% penicillin/streptomycin (Cellgro), 0.5% antibiotic/antimycotic (Life Technologies). The cells were examined for CD73, CD90 and CD105 as mesenchymal markers, CD31, CD34 and CD309 as vascular markers.

2.5. Flow cytometric analysis of hASCs and hDFs

Cells were detached with 0.05% trypsin/ethylenediamine tetra-acetic acid and washed with DPBS containing 2% FBS. They were then incubated with monoclonal antibodies conjugated with fluorescein isothiocyanate or phycoerythrin to detect mesenchymal markers (CD73, CD90, and CD105) or vascular markers [CD31, CD34 and CD309 (VEGFR2)] for 30 min at 4°C. Similarly-conjugated isotype controls (BD Biosciences) were used as negative controls. After incubation with the antibodies, cells were washed three times for 5 min each with DBPS containing 2% FBS, then analysed with the BD Accuri C6 flow cytometer.

2.6. Coculture and triculture experiments

Cells were plated onto bovine fibronectin (5 mg/mL diluted in cold distilled water; Sigma Aldrich)-coated 14 mm-diameter plastic coverslips that were placed in 24 well plates. All studies were performed on 2-cm^2 surfaces. Consistent nomenclature – thousands of NRVCM:hASC:HUVEC (or NRVCM:hDF:HUVEC) per cell culture well – is used to describe coculture and triculture cell plating densities throughout the manuscript. Therefore, for NRVCM:hASC cocultures, the HUVEC number is reported as zero. Likewise, in hASC:HUVEC experiments, the NRVCM number is reported as zero. The design of the protocol was based on keeping the total number of NRVCMs constant. The results of the coculture studies were used to obtain the input cell ratios for the triculture studies (Figure 1).

2.7. NRVCM-hASC/hDF coculture

NRVCMs were plated at a concentration of 500,000 cells in NRVCM medium containing 10% FBS. This number of NRVCMs was determined to form a confluent monolayer and was kept constant in all experiments. On the next day, different amounts of hASCs were plated on top of the NRVCMs resulting in ratios of 500:500:0, 500:250:0, 500:100:0, 500:50:0, and 500:0:0. An hASC-only well (0:500:0) was used as a negative control. Medium was switched to 2% FBS-containing medium, to reduce fibroblast proliferation, on the following day and refreshed every other day. On days 5–8, cells were assessed using optical mapping and were fixed with 4% paraformaldehyde for immunocytochemistry analysis. These studies were used to assess the maximum number of hASCs that could be added without causing significant changes in electrophysiology. To compare hASCs and hDFs, the studies were repeated for hDFs with cell ratios of 500:100:0 and 500:50:0.

2.8. hASC/hDF-HUVEC coculture

hASCs and HUVECs were mixed together in ratios of 0:100:100, 0:100:50, 0:100:20, 0:100:10, 0:50:50, 0:50:25, 0:50:10, and 0:50:5, and plated on coated cover slips. A HUVEC-only control 0:0:100 or 0:0:50 was included. The constructs were cultured *in vitro* for 7 days and fed every other day with EGM-2 (Lonza).

2.9. NRVCM /hASC/HUVEC triculture

NRVCMs were plated at a concentration of 500,000 cells in NRVCM media containing 10% FBS. On the following day, the media was removed, and coverslips were washed with DPBS prior to simultaneously plating hASCs and HUVECs to give final ratios of 500:100:50, 500:100:20, 500:100:10, 500:50:25, 500:50:10, 500:50:5. Two additional controls were included: no hASCs (500:0:50) and NRVCM only (500:0:0). Tri-cultures were fed EGM-2 (Lonza) media containing 2% heat-inactivated FBS (Sigma Aldrich), 20 μM glucose (Sigma Aldrich), 0.5% penicillin/streptomycin (Cellgro), and 0.5%

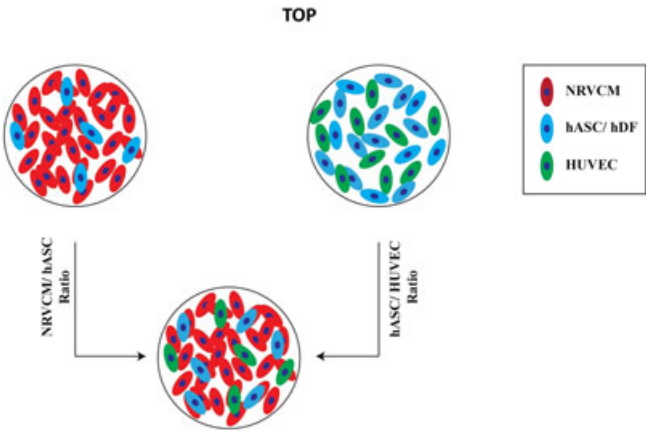

Figure 1. Schematic of experimental design. Coculture experiments were used to compare the effects of hASCs and hDFs on NRVCM electrophysiology and on vessel formation. The cell ratios obtained from coculture studies were used to inform the inputs for the NRVCM:hASC:HUVEC triculture system

antibiotic/antimycotic (Life Technologies). Culture media was refreshed every other day.

2.10. Optical mapping

Cocultures and tricultures containing NRVCMs were optically mapped using voltage-sensitive dye to record changes in their transmembrane voltage and visualize their excitation and repolarization (Tritthart, 2005). Optical mapping was performed on days 5–8. Coverslips containing cell monolayers were stained with 10 μM of the voltage-sensitive dye di-4-ANEPPS (Invitrogen), in Tyrode's solution for 10 min at 37°C while being protected from light.

After staining, the dye solution was removed, cells were washed with Tyrode's solution, and placed on a heated stage in Tyrode's solution with 5 μM blebbistatin to prevent motion artefacts due to contraction. Optical mapping was performed using a CMOS camera (MiCAM Ultima; Scimedia, Costa Mesa, CA, USA). Cells were electrically stimulated by placing a bipolar point electrode near the edge of the coverslip, out of the field of view of the camera, and paced starting at 0.5 Hz and incrementally increased by 0.5 Hz. At each new pacing rate, the cell monolayers were stimulated for 1 min to achieve steady state before an optical recording was taken. Pacing rate was increased until the ability of the sample to be captured at the pacing rate (i.e., action potential response with each pacing pulse) was lost or re-entrant spiral waves were formed.

2.11. Immunocytochemistry

On day 7, or after mapping, if applicable, cocultures and tricultures were fixed in 4% paraformaldehyde for 20 min at room temperature. After removing formaldehyde, cells were washed three times with DPBS for 30 min each time. Samples were permeabilized with 0.2% Triton X-100 (Sigma Aldrich) for 10 min and then blocked with 10% normal goat serum (Sigma Aldrich) in DPBS for 30 min. Coverslips were then incubated overnight at 4°C with: (1) mouse (Ms) anti-sarcomeric α-actinin [1:200] (Sigma Aldrich), rabbit (Rb) anti-connexin-43 [1:100] (Sigma Aldrich); (2) mouse anti-vimentin [1:200] (Dako) and TRITC conjugated phalloidin [1:50] (Sigma Aldrich); or (3) mouse anti-CD31 [1:250] (Sigma Aldrich). Primary antibodies were diluted in DPBS with 5% normal goat serum. Coverslips were washed three times with DPBS, then incubated overnight at 4°C with secondary antibodies DyLight 488-conjugated goat anti-mouse [1:200] and DyLight 649-conjugated goat anti-rabbit [1:200] (Jackson ImmunoResearch) that were diluted in 5% normal goat serum in DBPS. Samples were washed three times with DPBS and then incubated for 10 min at room temperature with DAPI [1:2000] (Sigma Aldrich) diluted in DPBS. Following the initial round of immunostaining, the samples stained with mouse anti-sarcomeric α-actinin and rabbit anti-connexin-43 were further blocked in 5% normal mouse serum in DPBS. Following blocking, samples were incubated with Cy3 conjugated mouse anti-α smooth muscle actin [1:400] (Sigma Aldrich) diluted in 5% normal mouse serum in DPBS incubated overnight at 4°C. Coverslips were subsequently washed three times with DPBS. Samples were mounted with mounting medium and imaged under a Zeiss Axio Observer inverted fluorescence microscope or a Zeiss LSM 510 confocal microscope with 5×, 20× and 40× objectives.

2.12. Image analysis

The 5× z-stacks were taken with 15-μm spacing, while 20× z-stacks had 3-μm spacing. Immunostained images were z-projected and thresholded in order to calculate vessel parameters including network length and junctions in the 3.24 mm^2 imaged region. Thresholded images were subsequently analysed with AngioQuant software to determine the total vessel length, area, and interconnectivity. Using a custom Image J macro, connexin 43 (Cx-43) stained images were thresholded,

and the number of stained foci was calculated. Cx-43 foci counts were divided by the area to report as Cx-43 foci/mm^2.

2.13. Statistical analysis

Quantitative data are reported as the mean ± the standard deviation. One-way ANOVA with Dunnett's *posthoc* test or Tukey's *posthoc* test was performed to determine statistical difference between testing groups. Differences were considered statistically significant at $^*p < 0.05$; $^{**}p < 0.01$; $^{***}p < 0.001$.

3. Results

3.1. Effect of hDFs and hASCs on electrophysiological parameters of cardiomyocytes

NRVCMs and hASCs were plated on sequential days, as described in the Methods, at varying ratios in order to determine the maximum number of hASCs that did not induce a statistically significant decrease in the conduction velocity or change in action potential duration when compared with NRVCM-only cultures. During testing, the action potential durations at 80% repolarization (APD_{80}) during 1 Hz pacing were significantly longer in the 500:500:0 (325 ± 42 ms) and 500:250:0 groups (268 ± 64 ms) relative to the 500:0:0 (cardiomyocyte only) group (168 ± 17 ms). APD_{80} of the other coculture ratios, 500:100:0 (201 ± 30 ms) and 500:50:0 (188 ± 13 ms) was not significantly different from that of the cardiomyocyte-only group (Figure 2A). Similar trends occurred with APD_{30} with values of 137 ± 26 ms (500:500:0), 83 ± 29 ms (500:250:0), 56 ± 9 ms (500:100:0), 50 ± 9 ms (500:50:0), and 48 ± 10 ms (500:0:0; Figure 2A; $n = 2–6$) . These trends held at other pacing rates as seen in Figure S1A. Maximum capture rate (MCR) decreased from roughly 4 ± 0.4 Hz (500:0:0) to 1.5 ± 0.03 Hz (500:500:0) with the addition of 500,000 hASCs. MCRs were statistically indistinguishable in the 500:250:0, 500:100:0, 500:50:0 and 500:0:0 groups but exhibited a statistically significant decrease in the 500:500:0 group (Figure S1C).

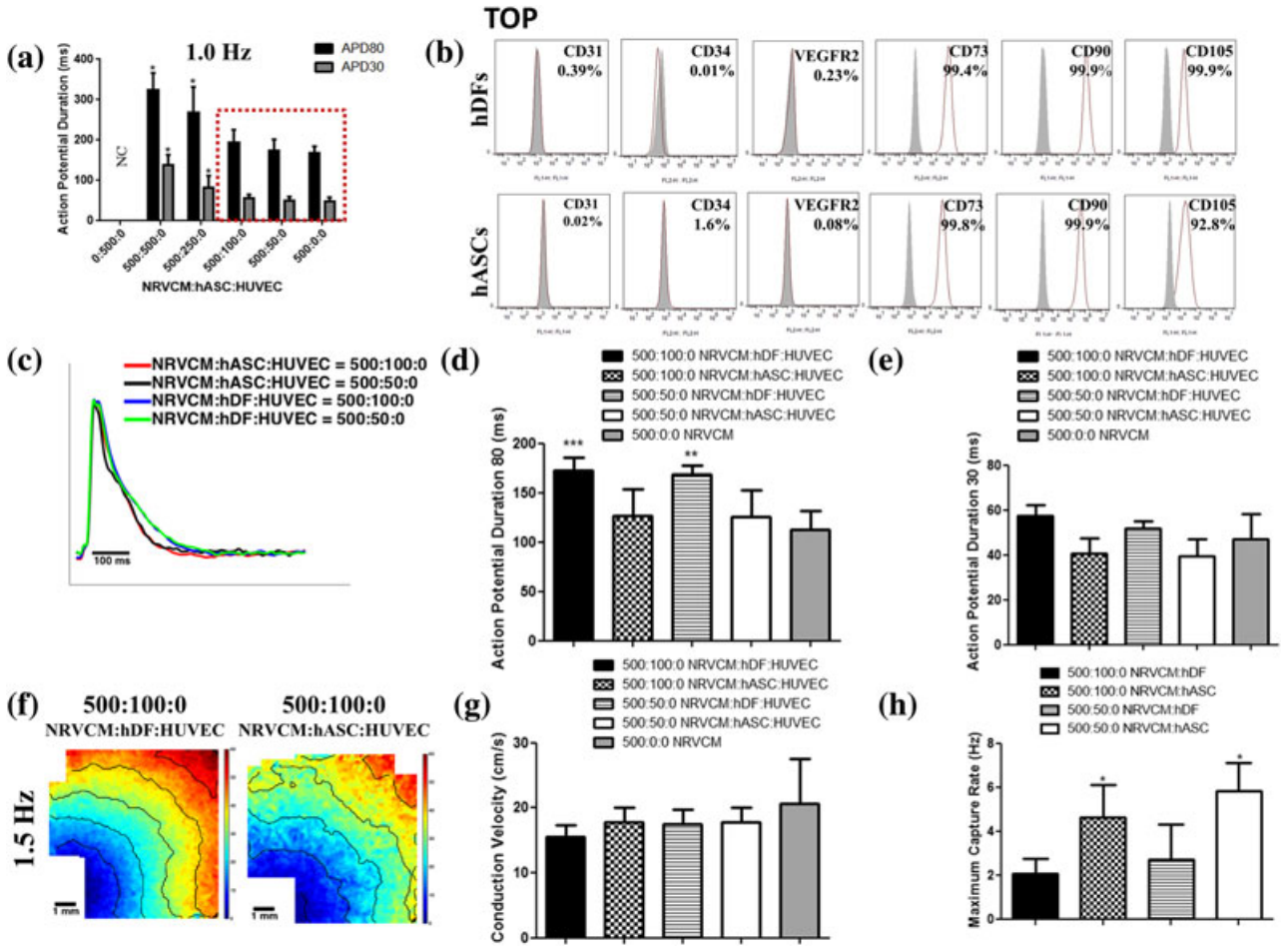

Figure 2. Effects of NRVCM:hASC and NRVCM:hDF ratios on electrophysiological function. (A) APD_{80} and APD_{30} values for different NRVCM:hASC:HUVEC ratios at a pacing rate of 1 Hz ($n = 3–5$). NC = not captured. * = $p < 0.05$ compared to 500:0:0. The red box indicates the groups that were used in subsequent studies as the electrophysiological parameters were not statistically different from NRVCMs only. (B) Phenotypic profile of P5 hDFs and P4 hASCs. Mesenchymal markers are CD73, CD90, and CD105, while vascular markers are CD31, CD34 and VEGFR2. (C) Action potential traces showing shorter durations in hASCs cocultures relative to hDF cocultures. (D) Comparison of APD_{80} among different experimental groups ($n = 5–6$), * = $p < 0.05$; ** $p < 0.01$; *** $p < 0.001$. (E) Comparison of APD_{30} among different experimental groups ($n = 5–6$). (F) Representative activation maps of selected cell ratios with isochrones 5 ms apart. (G) Comparison of conduction velocities among different experimental groups * = $p < 0.05$; ** $p < 0.01$; *** $p < 0.001$. (H) Maximum captured rates at identical ratios of NRVCM:hASC:HUVEC and NRVCM:hDF:HUVEC. * $p < 0.05$ compared to identical ratio of NRVCM:hDF:HUVEC

DOI: 10.1002/term

Based on these results, we compared the effects of coculturing NRVCMs with hDFs or hASCs using a subset of these cell ratios – 500:100:0 and 500:50:0 – as these groups did not exhibit significant increases in APD_{80} or APD_{30} compared to the cardiomyocyte-only cultures. Flow cytometry was performed to characterize the two cell populations. P5 hDFs and P4 hASCs were primarily positive for mesenchymal markers, CD73 (99.4%/99.8%), CD90 (99.9%/99.9%), and CD105 (99.9%/92.8%), respectively, and mostly negative for vascular markers CD31 (0.39%/0.02%), CD34 (0.01%/1.6%) and CD309/VEGFR2 (0.23%/0.08%; Figure 2B; $n = 3$). Immunocytochemistry revealed the presence of hDFs and hASCs in the cocultures via positive staining for vimentin, a marker of fibroblast-like cells (Figure S2A). APD_{80} and APD_{30} values were significantly shorter in the hASC cocultures compared to the hDF cocultures at both cell ratios. At 1.5 Hz, APD_{80} was 173 ± 12 ms (500:100:0) and 169 ± 15 ms (500:50:0) for NRVCM:hDF cocultures, compared to 126.5 ± 27 ms and 125.6 ± 27 ms for NRVCM:hASC cultures at 500:100:0 and 500:50:0 ratios, respectively (Figure 2C, D). The NRVCM-only control resulted in an APD_{80} of 112 ± 20 ms. APD_{30} ranged from 57 ± 5 ms in the 500:100:0 mixture containing hDFs to 40 ± 7 ms 500:50:0 containing hASCs, while APD_{30} was consistently near 47 ± 11 ms in the NRVCM only control group (500:0:0; Figure 2E). The conduction velocity (CV) at all pacing rates was maintained between 15 ± 2 and 19 ± 2 cm/s in both NRVCM:hDF and NRVCM:hASC cocultures with no significant differences between groups (Figure 2F,G). The NRVCM-only group (500:0:0) had CVs ranging from 15.7 ± 6 to 20.6 ± 7 cm/s at pacing rates from 0.5 to 2.0 Hz (Figure 2F,G; $n = 4$–6).

Cocultures with hASCs could be paced at faster rates (MCR = 5 ± 1.5 Hz for 500:100:0 and 6 ± 1.3 Hz for 500:50:0 ratio) than cocultures containing hDFs (2.08 ± 0.7 Hz and 3 ± 1.6 Hz, respectively, Figure 2 H). NRVCM:hASC cocultures exhibited increased expression of Cx-43, (500:100:0 and 500:50:0) as compared to NRVCM:hDF cocultures (Figure S2B, C). Although there was increased expression of Cx-43 in the NRVCM:hASC coculture relative to pure NRVCM cultures, there were no significant differences in conduction velocity compared to NRVCM:hDF cocultures. Other pacing rates exhibited similar trends (Figure S3).

3.2. Effect of hASC and HUVEC concentration on vessel formation

To determine the effects of cellular concentration on vessel assembly, hASCs and HUVECs were cocultured. Two hASC seeding densities were used – 100,000 cells/well or 50,000 cells/well – as these were the numbers of hASCs that did not significantly increase the APD_{80} of the cardiomyocytes in the NRVCM:hASC cocultures (Figure 2A). Various numbers of HUVECs were tested with these hASC concentrations. At a HUVEC density of 10,000 cells per well, vessel length increased when more hASCs were seeded (Figure 3B). For hASC:HUVEC cocultures containing 100,000 hASCs/well, vessel lengths and number of junctions both increased with decreasing amounts of HUVECs (Figure 3B,C). No vessels were formed in HUVEC-only controls. Staining in Figure 3 A shows that the endothelial cells have not yet formed vascular structures. For hASC:HUVEC cocultures with only 50,000 hASCs/well, the opposite results were observed, and vessel lengths and number of junctions both decreased with decreasing amounts of HUVECS (Figure 3B,C). hASCs in coculture with HUVECs appeared to take on a pericyte-like cell phenotype and stained positively for α-smooth muscle actin (Figure S4). Similar ratios were tested with dermal fibroblasts and resulted in vessels structures that did not develop like those in groups with hASCs (Figure S5).

3.3. Effect of triculture on cardiomyocyte electrophysiology

Based on the results of our initial studies, tricultures were established using only hASCs and not hDFs. The NRVCM:hASC:HUVEC ratios were determined by the previous coculture studies and included: (1) the amount of hASCs that did not significantly increase the APD_{80} (50,000 and 100,000); and (2) the ratios of hASCs:HUVECs that allowed for formation of robust vasculature. The study used six ratios of NRVCM:hASC:HUVEC in addition to no hASC controls (500:0:50) and NRVCM only controls (500:0:0). Samples were stained with CD31/PECAM-1 to indicate endothelial cell elongation and connectivity of endothelial cells. Groups that which formed vessel networks included 500:100:50, 500:100:20, 500:100:10, 500:50:25 and 500:50:10 ratios (Figure 4A). Samples were also stained for Cx-43 and CD31, revealing that Cx-43 positive loci were present near CD31-positive cells and, thus, that gap junctions, sites of the electrical connections of the cardiomyocytes, formed in close proximity to nascent vasculature (Figure 4A). Generally, vessel lengths decreased when the ratio of hASCs:HUVECs increased. There were no vessels detected in the ratios of 500:50:5, 500:0:50 and 500:0:0 (Figure 4 B). Vessel interconnectivity was determined by the number of junctions, which also tended to decrease when the ratio of hASCs:HUVECs increased (Figure 4C). The 500:50:25 ratio ultimately provided the best vessel assembly with the longest vessel length and supporting one of the higher amounts of interconnectivity extrapolated through number of junctions. In this group, average total vessel length was 70 mm per 3.24 mm^2, and vessel networks had an average of 454 junctions ($n = 3$).

Following triculture vessel characterization, electrophysiological properties of the tricultures were evaluated. There was no statistical difference in APD_{80}

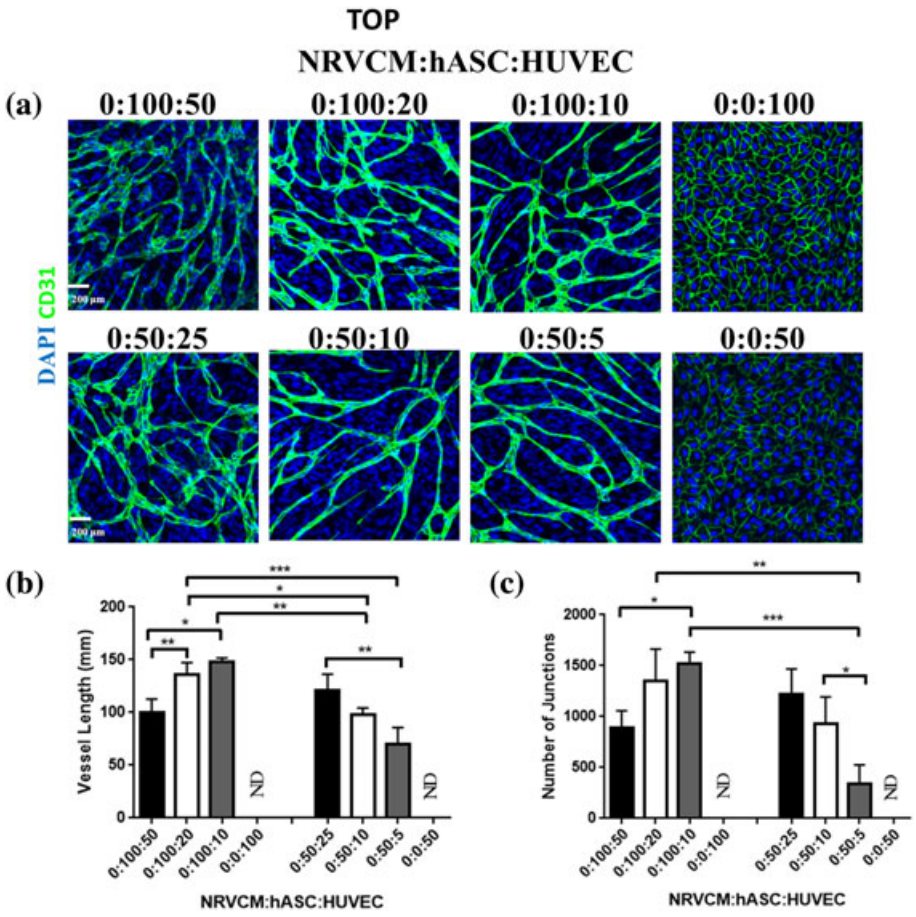

Figure 3. Effect of hASC:HUVEC ratios on vessel formation. (A) Immunofluorescent staining of CD31 positive vascular structures (green) and cell nuclei (DAPI; blue). Scale bar is 200 μm. Quantitation of vessel structure based on (B) length (n = 3) and (C) interconnectivity (n = 3). ND, not detected. $^{*}p < 0.05$; $^{**}p < 0.01$; $^{***}p < 0.001$

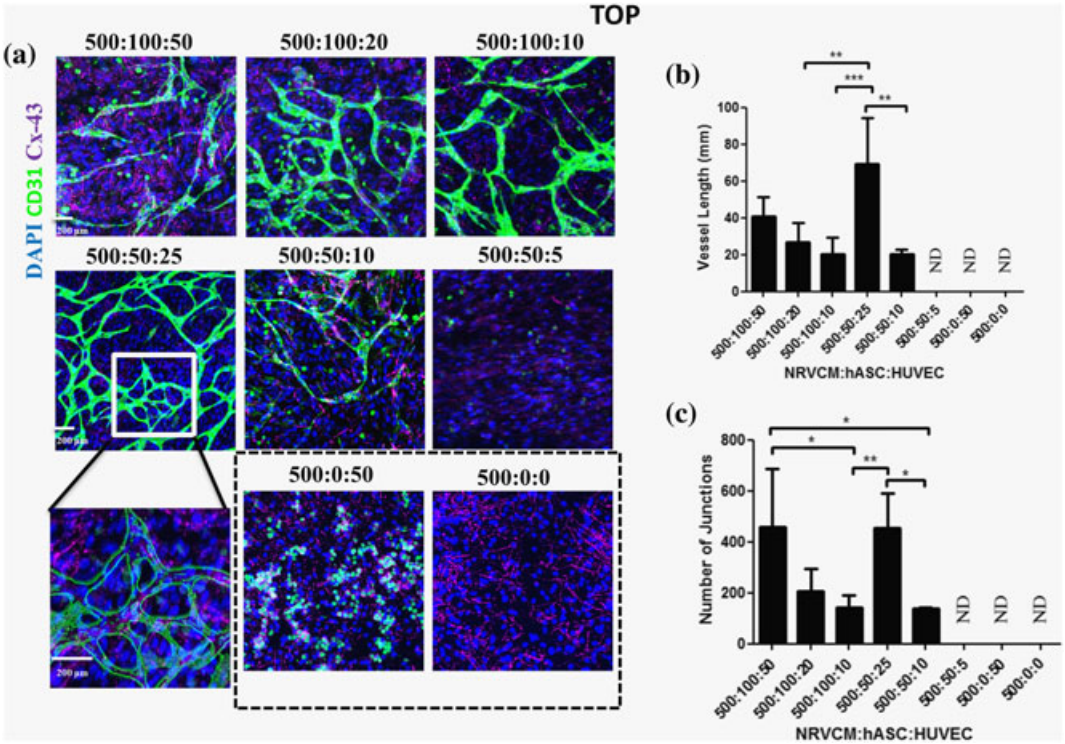

Figure 4. Vessel formation in triculture system. (A) Immunofluorescent staining of CD31 positive vascular structures (green), connexin-43 (Cx-43; purple), and cell nuclei (DAPI; blue). Scale bar is 200 μm. --- surrounds groups with no hASCs present that were cultured as controls. Quantitation of vessel structure based on (B) length (n = 4–6) and (C) interconnectivity (n = 4–6). (D) ND designates not detected. $^{*}p < 0.05$; $^{**}p < 0.01$; $^{***}p < 0.001$

of any of the tested triculture groups as compared to the cardiomyocyte-only control (120 ± 9 ms at 1.5 Hz pacing rate; n = 4–6; Figure 5A,B). Although no level of significance was reached, there appeared to be a trend of increasing APD_{80} with more hASCs present in cultures. The APD_{30} values were measured and calculated similarly. All triculture groups' APD_{30} values were not significantly different from the NRVCM only control (51 ± 5 ms at 1.5 Hz pacing rate; n = 4–6; Figure 5C). Similar trends were noted at the 2 Hz pacing rate for both APD_{80} and APD_{30} (Figure S6A,B, SV1, SV2).

CVs of the ratios 500:50:25 and 500:0:50 were not statistically different when compared to the NRVCM control (500:0:0), while all other groups had significantly lower CVs (25 ± 1 ms at 1.5 Hz pacing rate for control; Figure 5D,E). MCR was not significantly different between groups and fell between 6.7 ± 0.8 Hz (500:100:50) and 7.2 ± 0.2 Hz (500:0:0; n = 4–6; Figure 5F). Similar trends were noted at the 2 Hz pacing rate for CV (Figure S6C).

4. Discussion

Previous tricultures have used either embryonic stem cell-derived (ESC) cardiomyocytes or NRVCMs with endothelial cells that were either embryonic stem cell-derived (ESC-EC) (Caspi *et al.*, 2007; Lesman *et al.*, 2010), or mature, such as HUVECs (Caspi *et al.*, 2007). For example, Caspi *et al*. (2007) developed a triculture system with ESC cardiomyocytes, ESC-ECs and mouse embryonic fibroblasts cultured on poly(l-lactic-acid)/poly(lactide-coglycolide) PLLA/PLGA scaffolds. Mouse embryonic fibroblasts provided vascular stabilization, increased proliferation and reduced apoptosis of ESC-ECs, and the presence of stabilized vasculature correlated with increased cardiomyocyte proliferation. Additionally, Iyer *et al*. (2009a, b, 2012) investigated simultaneous seeding and sequential seeding of triculture systems. Simultaneous seeding of all three cell types impeded the development of gap junctions between cardiomyocytes and resulted in the presence of rounded cardiomyocytes with no ability to contract. Just as importantly, simultaneous seeding of cardiomyocytes with endothelial cells and fibroblasts resulted in endothelial cells that did not elongate to form vessel-like structures. However, when cardiomyocytes were seeded first and allowed to attach and form electrical connections with each other prior to adding other cell types, they elongated and expressed the gap junction protein Cx-43, and cardiac troponin. Thus, a sequential seeding approach was used, where a high density of NRVCMs was plated into each well 1 day prior to the addition of coculture or triculture cells. In hASC-HUVEC cocultures, cells were seeded simultaneously. The main objectives of this study were to assess the potential for using hASCs as a suitable cell source for vascular stabilization in tricultures with HUVECs and NRVCMs and to determine the appropriate cell ratios required for the development of vascularized cardiac tissues. The key success criteria were that the tricultures should be capable of maintaining similar electrophysiological function (maintenance of repolarization rates and maximum capture rates) compared to NRVCM-only controls and simultaneously demonstrate the presence of well-developed vascular structures.

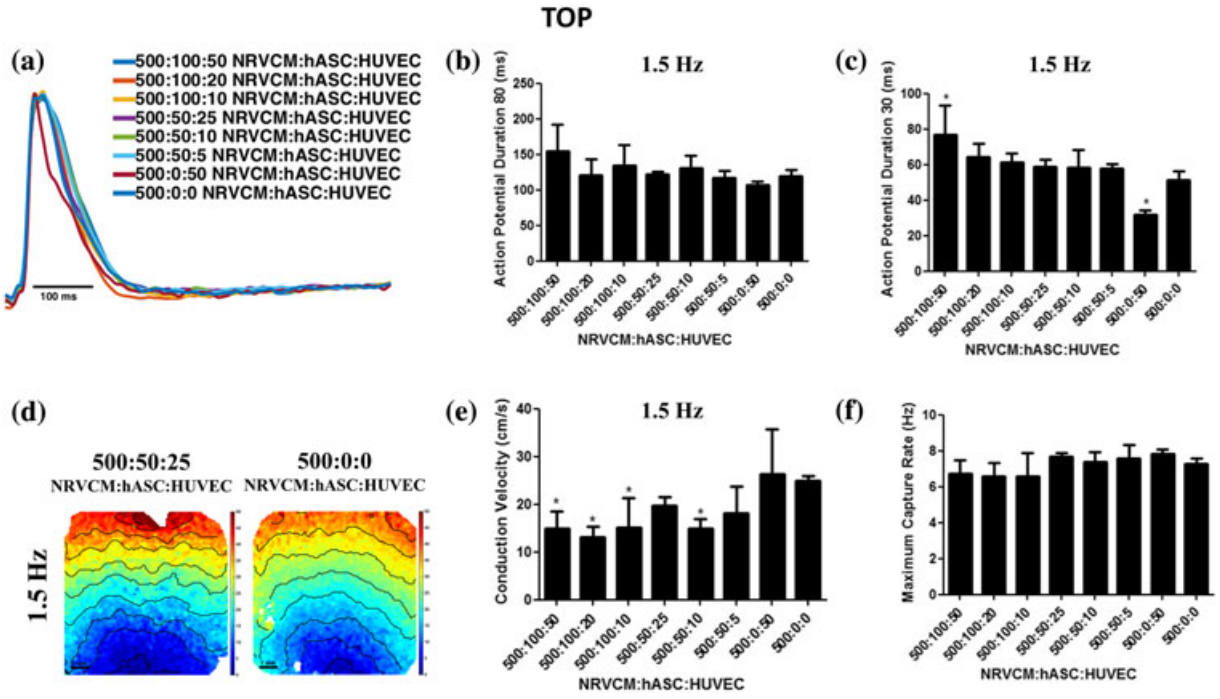

Figure 5. Effects of triculture ratios on electrophysiological function. Effects of triculture ratios on (A) Representative action potential traces of all selected ratios; (B) APD_{80} (n = 4–6); (C) APD_{30} (n = 4–6). (D) Activation maps of selected ratios with isochromes 5 ms apart. (E) conduction velocity at 1.5 pacing rates (n = 4–6). (F) Assessment of maximum capture rate for various triculture ratios. *$p < 0.05$ compared to the cardiomyocyte only group (500:0:0)

DOI: 10.1002/term

Previous studies have also used hDFs with endothelial cells to establish *in vitro* models of vasculogenesis (Liu *et al.*, 2009; Sorrell *et al.*, 2007), although, more recently, studies of vascular coculture have shown that hASCs outperform hDFs and SMCs as vascular support cells (Merfeld-Clauss *et al.*, 2010). Previously published studies of triculture systems with NRVCM and endothelial cells used primary cardiac fibroblasts (Iyer *et al.*, 2009b) and embryonic fibroblasts (Caspi *et al.*, 2007) as vascular support cells. Therefore, this study compared hASCs to the hDF cells to incorporate the functionality of the previous triculture systems with the improved vascular support of hASCs. Previous studies have also demonstrated the potential of hASCs to act as cardiomyocyte support cells (Choi *et al.*, 2010) as well as perivascular cells to maintain the stability of nascent vascular structures formed by endothelial cells (Hutton *et al.*, 2012, Merfeld-Clauss *et al.*, 2014). To determine an upper limit of their role as support cells, this study probed the maximum concentration of hASCs that could be added to pure cultures of NRVCMs before the electrophysiological properties of the NRVCMs would be significantly compromised. Typically, cocultures of cardiomyocytes with fibroblasts or fibroblast-like cells in culture have increased action potential durations and reduced conduction velocities (McSpadden *et al.*, 2009). Similarly, NRVCMs cocultured with either hASCs or hDFs at concentrations above a threshold level had similar CVs but shorter action potential durations than NRVCM-only control groups. hASC concentrations that exceeded 20% of the cardiomyocytes reduced the maximum capture rates, increased the duration of action potentials, and reduced the rates of conduction (Figure S1). This led to further studies with NRVCM:hASC cocultures at ratios of 20% or less (500:100:0 and 500:50:0). When hASCs were directly compared with hDFs, hDFs had significantly lower maximum capture rates and significantly longer repolarization times at equivalent concentrations. hASCs thus proved to be a more attractive cell source than hDFs for triculture systems. It is interesting to note that cocultures of NRVCMs with hASCs exhibited increased Cx-43 expression, relative to NRVCM:hDF cocultures (Figure S2). However, further experiments are needed to identify the exact underlying mechanisms for improved outcomes with hASCs as opposed to hDFs.

To assess the effect of hASCs on the development of vascular structures, they were cocultured with HUVECs. Prior studies have reported that EPCs or HUVECs cocultured with hASCs developed robust vascular structures in cell monolayers (Merfeld-Clauss *et al.*, 2010, 2014). These findings indicated that hASCs can act as vascular mural cells that contribute to the development and stabilization of cord-like vessel structures. Mechanistically, hASCs promote vascular development by paracrine signalling (Crisan *et al.*, 2008; Verseijden *et al.*, 2010), including growth factor secretion (Traktuev *et al.*, 2008), and direct cell-cell contact (for stabilization) with the endothelial cells (Hutton *et al.*, 2012; Merfeld-Clauss *et al.*, 2010, 2014; Traktuev *et al.*, 2008). Vessel development occurred at all tested ratios of hASC:HUVEC cocultures. In these studies, the initial numbers of hASCs were kept constant at 100,000 cells/well and 50,000 cells/well to be consistent with the hASC numbers that did not significantly alter APD, CV and MCR in the NRVCM: hASC studies. There were measurable differences in the total vessel length and interconnectivity among the various ratios. However, no general trends emerged: when 100,000 hASCs/well were used, lower numbers of endothelial cells resulted in longer vascular structures, while the opposite was true when 50,000 hASCs/well were used. However, HUVECs were unable to form network structures in the absence of hASCs. When hDFs were used *in lieu* of hASCs, the ability of HUVECs to form vascular structures was significantly lower (Figure S3). This study did not assess the mechanistic reason for this difference in proangiogenic potential of hASCs and hDFs. However, prior studies suggest that hASCs may secrete higher concentrations of VEGF than hDFs (Blasi *et al.*, 2011). Another study compared cocultures of EPCs and hASCs to cocultures of EPCs and hDFs, and found that total tube length and branch points were significantly decreased in the dermal fibroblast group (Merfeld-Clauss *et al.*, 2010). Note that the vascular structures developed in our cultures are two-dimensional and may not contain lumens. However, the data gleaned from this study provide fundamental insights for subsequent studies in 3D scaffolds and hydrogel systems.

These two coculture studies of NRVCM:hASC and hASC:HUVEC were used to provide starting cell ratios for the triculture system. Based on the superior performance of hASCs relative to hDFs in both NRVCM and HUVEC coculture systems, were did not assess the efficacy of hDF in the triculture studies. The concentrations of NRVCMs were maintained constant at 500,000 cells/well and plated a day prior to the addition of hASCs and HUVECs. Based on NRVCM:hASC coculture studies, only two concentrations of hASCs were tested (50,000 cells/well and 100,000 cells/well). Three hASC:HUVEC ratios were assessed (0:100:50/ 0:50:25; 0:100:20/0:50:10, and 0:100:10/0:50:5), and consequently, HUVEC seeding densities varied from 5000 cells/well up to 50,000 cells/well. The six resulting ratios for the triculture were compared to cultures of pure NRVCMs. Interestingly, the relative cell numbers in the tricultures do not reflect the reported cell ratio for the native myocardium. The total number of NRVCMs found in our monolayer cultures is necessary for high levels of connectivity possibly due to the limited proliferative potential of NRVCMs compared to hASCs and HUVECs (Simpson and Savion, 1982). We found that vessels developed in all triculture groups except for 500:50:5, where the number of endothelial cells may have been too low. Likewise, the absence of hASCs from the cultures (500:0:50) resulted in no vascular structures forming indicating that the hASCs were essential for vascular morphogenesis in these

cultures. Vessel development was highest at the ratio of 500:50:25. While previous studies suggest that VEGF-VEGFR2 signalling correlates with increased Cx-43 expression and maintenance of electrophysiological function (i.e. excitation threshold and maintenance of maximum capture rate) (Iyer *et al.*, 2012), our tricultures maintained relatively similar conduction velocities and maximum capture rates, however, increased concentrations of non-cardiomyocytes resulted in increased repolarization times.

5. Conclusion

The high metabolic demands of the myocardium require robust vascularization to maintain survival/viability, maintain force of contraction and prevent necrosis due to ischemia in deeper layers of the engineered tissue. Therefore, a tissue engineered cardiac triculture must include a ratio of cells that maximizes formation of nascent vasculature without compromising electrophysiological function of the graft. Multiple cell types are essential for complex tissue assembly, but they should not interrupt the formation of functional cardiac syncytium. In this study, we demonstrated that a 500:50:25 ratio of NRVCM:hASC:HUVEC facilitated the development of a graft with unaltered electrophysiological parameters with dense capillary-like vessel structures. The success of this triculture system was supported by the use of hASCs, which played a critical role as a vascular mural cell that did not impede the electrical activity of cardiomyocytes, as fibroblasts do. Additionally, hASCs performed significantly better than dermal fibroblasts in forming vascular networks and maintaining electrophysiological properties that were similar to cardiomyocyte only controls. These findings suggest that hASCs may be a highly suitable cell source for use in future triculture studies for engineering functional, vascularized myocardium.

Disclosure statement

No competing financial interest exists.

Acknowledgements

We would like to thank Dr Jeff Gimble for his help with hASC preparation. We would like to thank Renjun Zhu for assistance with optical mapping data analysis. Use of the Zeiss LSM 510 was made possible by the Microscopy and Imaging Core Module of the Wilmer Eye Institute Core Grant P30-EY001765.

References

Baum J, Duffy HS. 2011; Fibroblasts and myofibroblasts: what are we talking about? *J Cardiovasc Pharmacol* **57**(4): 376–9.

Blasi A, Martino C, Balducci L *et al*. 2011; Dermal fibroblasts display similar phenotypic and differentiation capacity to fat-derived mesenchymal stem cells, but differ in anti-inflammatory and angiogenic potential. *Vasc Cell* **3**: 5.

Blazeski A, Kostecki GM, Tung L. 2015; Engineered heart slices for electrophysiological and contractile studies. *Biomaterials* **55**: 119–128.

Brutsaert DL. 2003; Cardiac endothelial-myocardial signaling: its role in cardiac growth, contractile performance, and rhythmicity. *Physiol Rev* **83**: 59–115.

Caspi O, Lesman A, Basevitch Y *et al*. 2007; Tissue engineering of vascularized cardiac muscle from human embryonic stem cells. *Circ Res* **100**: 263–272.

Chen X, Aledia AS, Popson SA *et al*. 2010; Rapid anastomosis of endothelial progenitor cell-derived vessels with host vasculature is promoted by a high density of cotransplanted fibroblasts. *Tissue Eng Part A* **16**: 585–594.

Choi YS, Dusting GJ, Stubbs S *et al*. 2010; Differentiation of human adipose-derived stem cells into beating cardiomyocytes. *J Cell Mol Med* **14**: 878–89.

Corselli M, Chin CJ, Parekh C *et al*. 2013; Perivascular support of human hematopoietic stem / progenitor cells. *Blood* **121**(15): 2891–2901.

Crisan M, Corselli M, Chen WCW *et al*. 2012; Perivascular cells for regenerative medicine. *J Cell Mol Med* **16**: 2851–2860.

Crisan M, Yap S, Casteilla L *et al*. 2008; A perivascular origin for mesenchymal stem cells in multiple human organs. *Cell Stem Cell* **3**: 301–313.

Dubois SG, Floyd EZ, Zvonic S *et al*. 2008; Isolation of human adipose-derived stem cells from biopsies and liposuction specimens. *Methods Mol Biol* **449**: 69–79.

Freiman A, Shandalov Y, Rozenfeld D *et al*. 2016; Adipose-derived endothelial and mesenchymal stem cells enhance vascular network formation on three-dimensional constructs *in vitro*. *Stem Cell Res Ther* **7**: 5.

Hirt MN, Hansen A, Eschenhagen T. 2014; Cardiac tissue engineering: state of the art. *Circ Res* **114**: 354–367.

Hutton DL, Logsdon EA, Moore EM *et al*. 2012; Vascular morphogenesis of adipose-derived stem cells is mediated by heterotypic cell-cell interactions. *Tissue Eng Part A* **18**: 1729–1740.

Iyer RK, Chiu LLY, Radisic M. 2009a; Microfabricated poly(ethylene glycol) templates enable rapid screening of triculture conditions for cardiac tissue engineering. *J Biomed Mater Res A* **89**: 616–31.

Iyer RK, Chui J, Radisic M. 2009b; Spatiotemporal tracking of cells in tissue-engineered cardiac organoids. *J Tissue Eng Regen Med* **3**: 196–207.

Iyer RK, Odedra D, Chiu LLY *et al*. 2012; Vascular endothelial growth factor secretion by nonmyocytes modulates connexin-43 levels in cardiac organoids. *Tissue Eng Part A* **18**: 1771–1783.

Jackman CP, Shadrin IY, Carlson AL *et al*. 2015; Human cardiac tissue engineering: from pluripotent stem cells to heart repair. *Curr Opin Chem Eng* **7**: 57–64.

Kawamura M, Miyagawa S, Fukushima S *et al*. 2013; Enhanced survival of transplanted human induced pluripotent stem cell-derived cardiomyocytes by the combination of cell sheets with the pedicled omental flap technique in a porcine heart. *Circulation* **128**: S87–94.

Koh YJ, Koh BI, Kim H *et al*. 2011; Stromal vascular fraction from adipose tissue forms profound vascular network through the dynamic reassembly of blood endothelial cells. *Arterioscler Thromb Vasc Biol* **31**: 1141–1150.

Kohl P, Camelliti P, Burton FL *et al*. 2005; Electrical coupling of fibroblasts and myocytes: relevance for cardiac propagation. *J Electrocardiol* **38**: 45–50.

Lesman A, Gepstein L, Levenberg S. 2010; Vascularization shaping the heart. *Ann N Y Acad Sci* **1188**: 46–51.

Liau B, Christoforou N, Leong KW *et al*. 2011; Pluripotent stem cell-derived cardiac tissue patch with advanced structure and function. *Biomaterials* **32**: 9180–7.

Liu H, Kennard S, Lilly B. 2009; NOTCH3 expression is induced in mural cells through an autoregulatory loop that requires Endothelial-expressed JAGGED1. *Circ Res* **104**: 466–475.

McSpadden LC, Kirkton RD, Bursac N. 2009; Electrotonic loading of anisotropic cardiac monolayers by unexcitable cells depends on connexin type and expression level. *Am J Physiol Cell Physiol* **297**: C339–C351.

Merfeld-Clauss S, Gollahalli N, March KL *et al*. 2010; Adipose tissue progenitor cells directly interact with endothelial cells to induce vascular network formation. *Tissue Eng Part A* **16**: 2953–2966.

Merfeld-Clauss S, Lupov IP, Lu H *et al*. 2014; Adipose stromal cells differentiate along a smooth muscle lineage pathway upon endothelial cell contact via induction of activin A. *Circ Res* **115**: 800–809.

Poll D, Parekkadan B, Borel Rinkes IHM *et al*. 2008, Mesenchymal stem cell therapy for protection and repair of injured vital organs. *Cell Mol Bioeng* **1**: 42–50.

Porter KE, Turner NA. 2009; Cardiac fibroblasts: at the heart of myocardial remodeling. *Pharmacol Ther* **123**: 255–278.

Shadrin IY, Yoon W, Li L *et al*. 2015; Rapid fusion between mesenchymal stem cells and cardiomyocytes yields electrically active, non-contractile hybrid cells. *Sci Rep* **5**: 12043.

Simpson P, Savion S. 1982; Differentiation of rat myocytes in single cell cultures with and without proliferating nonmyocardial cells. Cross-striations, ultrastructure, and chronotropic response to isoproterenol. *Circ Res* **50**: 101–16.

Sorrell JM, Baber MA, Caplan AI. 2007; A self-assembled fibroblast-endothelial cell co-culture system that supports *in vitro* vasculogenesis by both human umbilical vein endothelial cells and human dermal microvascular endothelial cells. *Cells Tissues Organs* **186**(3): 157–168.

Takeda N, Manabe I, Uchino Y *et al*. 2010; Cardiac fibroblasts are essential for the adaptve response of the murine heart to pressure overload. *J Clin Densitom* **120**(1): 1254–1265.

Tandon V, Zhang B, Radisic M, *et al*. 2013; Generation of tissue constructs for cardiovascular regenerative medicine: from cell procurement to scaffold design. *Biotechnol Adv* **31**: 722–735.

Thompson SA, Blazeski A, Copeland CR *et al*. 2014; Acute slowing of cardiac conduction in response to myofibroblast coupling to cardiomyocytes through N-cadherin. *J Mol Cell Cardiol* **68**: 29–37.

Toraason M, Luken ME, Breitenstein M *et al*. 1989; Comparative toxicity of allylamine and acrolein in cultured myocytes and fibroblasts from neonatal rat heart; *Toxicology* **56**: 107–117.
Traktuev DO, Merfeld-Clauss S, Li J *et al*. 2008; A population of multipotent CD34-positive adipose stromal cells share pericyte and mesenchymal surface markers, reside in a periendothelial location, and stabilize endothelial networks. *Circ Res* **102**: 77–85.
Tritthart HA. 2005; Optical techniques for the recording of action potentials. In: Practical Methods in Cardiovascular Research. Springer, Berlin, 215–232.
Verseijden F, Posthumus-van Sluijs SJ, Pavljasevic P *et al*. 2010; Adult human bone marrow- and adipose tissue-derived stromal cells support the formation of prevascular-like structures from endothelial cells *in vitro*. *Tissue Eng Part A* **16**: 101–114,
Yoshimura K, Suga H, Eto H. 2009; Adipose-derived stem/progenitor cells: roles in adipose tissue remodeling and potential use for soft tissue augmentation. *Regen Med* **4**: 265–273.

Supporting information

Additional Supporting Information may be found online in the supporting information tab for this article.

Figure 1. Effect of NRVCM:hASC ratios on electrophysiological function at different pacing frequencies. (A) APD_{80} and APD_{30} values (n = 3–5). (B) Conduction velocities (n = 3–5). (C) Maximum capture rates. * $p < 0.05$; ** $p < 0.01$; *** $p < 0.001$ compared to the cardiomyocyte only group (500:0:0). (D) Representative action potential traces of all selected ratios.
Figure 2. Immunofluorescent staining of NRVCM:hASC and NRVCM:hDF cocultures. (A) Immunofluorescent staining of vimentin (green), F-actin (red), and DAPI (blue) in cocultures. (B) Immunofluorescent staining of αSMA (red), connexin 43 (purple), α-actinin (green) and DAPI (blue) in cocultures. Scale bar is 200 μm. (C) Quantification of connexin43 (Cx-43) expression.
Figure 3. Comparison of the electrophysiological impact of hASCs and hDFs cocultured with NRVCMs. (A) APD_{80} values of NRVCM:hDF and NRVCM:hASC cocultures at various pacing rates. (B) APD_{30} values of NRVCM:hDF and NRVCM:hASC cocultures at various pacing rates. (C) Conduction velocity values of NRVCM:hDF and NRVCM:hASC cocultures at various pacing rates. NC = not captured. * = $p < 0.05$ compared to identical ratio of NRVCM:hDF:HUVEC (n = 5–6).
Figure 4. hASC:HUVEC coculture results in pericyte-like cell phenotype in hASC. Immunofluorescent staining of CD31 (green), αSMA (red), and DAPI (blue) showing pericyte-like differentiation of hASCs in close proximity to CD31 cells. Scale bar is 200 μm.
Figure 5. Effect of hDF:HUVEC ratios on vessel formation. Immunofluorescent staining of CD31 positive vascular structures (green) and cell nuclei (DAPI; blue). Scale bar is 200 μm.
Figure 6. Electrophysiological properties of various triculture ratios paced at 2 Hz. (A) APD_{80} values of NRVCM:hASC:HUVEC tricultures at 2 Hz. (B) APD_{30} values of NRVCM:hASC:HUVEC tricultures at 2 Hz. (C) Conduction velocity values of NRVCM:hASC:HUVEC tricultures at 2 Hz. * = $p < 0.05$ compared to 500:0:0 control (n = 4–6)
Video 1. Video of action potential propagation for triculture ratio 500:50:25. NRVCM:hASC:HUVEC tricultures at the ratio of 500:50:25 had conduction velocity values of 18.8 ± 1.42 cm/s, APD_{80} values of 120 ± 4.95 ms, and APD_{30} values of 53 ± 4.60 ms. Maximum captured rate was 7.68 ± 0.23 Hz.
Video 2. Video of action potential propagation for triculture ratio 500:0:0. NRVCM only cultures (500:0:0) exhibited similar electrophysiological properties as the 500:50:25 group. They had conduction velocity values of 23.48 ± 1.93 cm/s, APD_{80} values of 117 ± 7.56 ms, and APD_{30} values of 47 ± 4.22 ms. Maximum captured rate was 7.84 ± 0.23 Hz.